Journal of Alloys and Compounds 508 (2010) 14–19

Contents lists available at ScienceDirect

Journal of Alloys and Compounds

journal homepage: www.elsevier.com/locate/jallcom

Tunable Curie temperatures in Gd alloyed Fe–B–Cr magnetocaloric materials

J.Y. Law[a], R.V. Ramanujan[a,*], V. Franco[b]

[a] School of Materials Science and Engineering, Nanyang Technological University, Singapore 639798, Singapore
[b] Dpto. Física de la Materia Condensada, ICMSE-CSIC, Universidad de Sevilla, P.O. Box 1065, 41080 Sevilla, Spain

ARTICLE INFO

Article history:
Received 8 July 2010
Received in revised form 2 August 2010
Accepted 4 August 2010
Available online 20 August 2010

Keywords:
Amorphous materials
Rare earth alloys and compounds
Rapid-solidification
Quenching
Magnetocaloric
Magnetic measurements

ABSTRACT

The magnetocaloric effect of $Fe_{80-x}B_{12}Cr_8Gd_x$ ($x = 1, 2, 3, 5, 8, 10, 11$) amorphous alloys was studied. Gd addition increases the thermal stability of the alloy and allows tuning the Curie temperature (T_C). A linear relationship between the magnetic entropy change and the magnetic moment of the alloy was observed. The experimental values of magnetic field dependence of the magnetic entropy change were consistent with a phenomenological universal curve. The maximum magnetic entropy change, for $x = 1$, was ~33% larger than $Fe_{80}B_{12}Cr_8$, the refrigerant capacity (*RC*) is ~29% larger than $Gd_5Si_2Ge_{1.9}Fe_{0.1}$ and within 10% of $Fe_{82.5}Zr_7B_4Co_{2.75}Ni_{2.75}Cu_1$ which is the best Fe-based amorphous MCM to date. The tunable T_C can be used to increase *RC* and the temperature span of layered multi-composition magnetocaloric regenerators.

1. Introduction

The search for new magnetocaloric materials (MCM) is attracting considerable attention recently, since their practical applications are in the energy efficient environmentally friendly magnetic refrigeration technologies [1–12]. This technology exploits the magnetocaloric effect (MCE), which corresponds to the temperature change of a magnetic material when adiabatically subjected to a varying magnetic field. Magnetic cooling is a promising alternative to classical vapor compression–expansion refrigeration since it is energy efficient, does not require compressors and does not use ozone-depleting gases [1,2,6,7,9,12]. A large MCE is obtained for a large change in saturation magnetization when the temperature is altered. This is achieved by a magnetic or magneto-structural phase transition in the vicinity of the working temperature. MCM can be divided into two classes based on the type of phase transitions: first order magneto-structural phase transition (FOMT) and second order magnetic phase transition (SOMT). FOMT materials, also known as giant magnetocaloric effect (GMCE) materials, exhibit larger peak magnetic entropy change ($\left|\Delta S_M^{pk}\right|$) due to their magneto-crystallographic phase transition, but this is accompanied by undesirable thermal hysteresis. SOMT materials usually display lower $\left|\Delta S_M^{pk}\right|$, broader $\Delta S_M(T)$ peaks and reduced hysteresis, resulting in enhanced refrigerant capacity (*RC*). This, facilitates an increase in operating frequency of magnetic refrigerators, hence SOMT materials are still preferred as the MCM in refrigerator prototypes. Gadolinium, a SOMT material, is the *de facto* reference material for MCE because its Curie temperature (T_C) is close to room temperature and it exhibits a large magnetocaloric response. Gd is also the base for crystalline compounds, such as $Gd_5Si_2Ge_2$ [13] and $Gd_5Si_2Ge_{1.9}Fe_{0.1}$ [14], which exhibit GMCE. However, the high price of Gd and its low corrosion resistance has necessitated the search for affordable materials which are suitable for room temperature magnetic refrigeration. Hence there is considerable interest in developing soft magnetic amorphous alloys for MCE applications.

The advantages of soft magnetic amorphous alloys for magnetic refrigeration applications include low magnetic hysteresis, high electrical resistivity (which will lower eddy current heating arising from the varying magnetic field), enhanced corrosion resistance, good mechanical properties and the possibility of tuning the Curie temperature by alloying [15–19]. Among the soft magnetic MCM, Fe-based amorphous alloys exhibit competitive advantages such as having abundant raw materials and low fabrication cost. Nanoperm type alloys display the highest MCE among Fe-based amorphous alloys, but usually at elevated temperatures [16,19,20]. $Fe_{80}B_{12}Cr_8$ amorphous alloys were recently reported to exhibit promising MCE near room temperature and the corrosion resistance is enhanced by Cr [21]. Other studies show that rare earth based amorphous alloys exhibit large magnetocaloric response, but their working temperatures are much lower than room temperature [22–28].

* Corresponding author. Tel.: +65 67904342; fax: +65 67909081.
E-mail address: Ramanujan@ntu.edu.sg (R.V. Ramanujan).

0925-8388/$ – see front matter © 2010 Elsevier B.V. All rights reserved.
doi:10.1016/j.jallcom.2010.08.049

MCM exhibit maximum MCE around their T_C. Regenerators consisting of layers of MCM, enhance both operating temperature range and *RC* [29]. Thus, composite MCM with increasing T_C are the optimum materials for active regenerative refrigerators [6,12,29–31]. Hence, with the aim of tuning the Curie temperature of Fe–B–Cr alloys around room temperature, we examined the influence of Gd addition on the $Fe_{80}B_{12}Cr_8$ alloy. The experimental results were also found to be consistent with a phenomenological universal curve developed to predict the magnetic entropy change. We find that the Curie temperature increases as Gd content increases, these alloys can be used as multilayer MCM to increase the temperature range and *RC* of magnetic refrigeration devices.

2. Experimental

Buttons of nominal composition $Fe_{80-x}B_{12}Cr_8Gd_x$ (x = 1, 2, 3, 5, 8, 10 and 11) were prepared by arc melting high-purity elemental constituents (Fe, Strem Chemicals, 99.95%; Gd, Alfa Aesar, 99.99%; Cr, Sigma–Aldrich, 99.99%; B, LTS (chemical), 99.99%) in argon atmosphere. The buttons were subsequently melt spun into ribbons (with thickness and width of 10–20 μm and ~1 mm, respectively) by single roller melt spinning (Edmund Bühler GmbH., Melt Spinner SC) under an argon atmosphere at a surface speed of 44 m/s. The ribbons will be denoted by their Gd content as Gd1, Gd2, Gd3, Gd5, Gd8, Gd10 and Gd11.

The structure of the ribbons was characterized by X-ray diffraction (Shimadzu 6000 diffractometer, Cu Kα radiation) and by transmission electron microscopy (JEOL JEM 2010 with C_S = 0.5 mm). Compositional analysis was performed using energy dispersive X-ray spectroscopy (EDS). The thermal stability of the ribbons was studied by a NETZSCH DSC-404 differential scanning calorimeter (DSC), using a 10 K min^{-1} scan.

The field dependence of magnetization was measured by a Lakeshore 7400 series vibrating sample magnetometer (VSM).

3. Results and discussion

The amorphous character of the ribbons was verified by X-ray diffraction and bright field images with their corresponding bright halos in the selected area diffraction patterns. The EDS results also showed good agreement with the nominal composition. The devitrification behavior of the studied alloys was studied by DSC (Fig. 1). For low Gd content, onset temperature of crystallization (T_x) increases as Gd content in the alloy increases, reaching a plateau at around 8 at.% Gd. This trend suggests that the thermal stability of the alloys is enhanced according to the confusion principle [32].

The magnetic entropy change (ΔS_M) due to the application of a magnetic field (H) was calculated from the integration of the temperature (T) and field dependent magnetization curves according

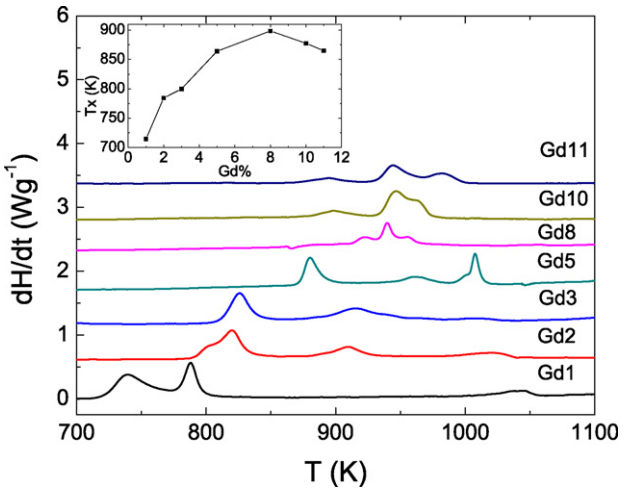

Fig. 1. Main panel: DSC thermographs of as-spun $Fe_{80-x}Gd_xCr_8B_{12}$ ribbons measured at a heating rate of 10 K min^{-1}. Inset: compositional dependence of onset of crystallization temperature.

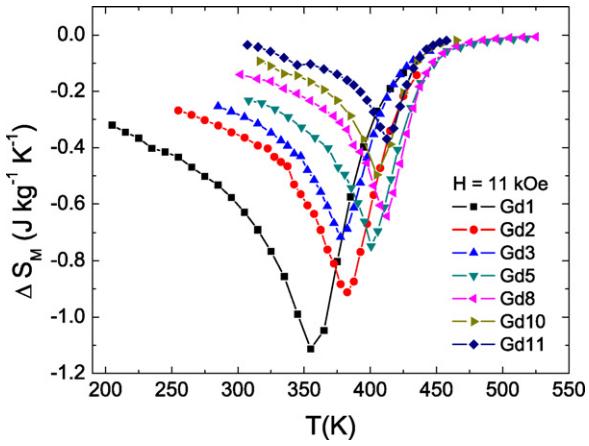

Fig. 2. Values of magnetic entropy change calculated from VSM magnetization data.

to the equation:

$$\Delta S_M = \int_0^H \left(\frac{\partial M}{\partial T}\right)_H dH. \quad (1)$$

There are several definitions in the literature for the refrigerant capacity (*RC*), which is a measure of the heat which can be transferred between the hot and cold reservoirs [3,33]. In this work, we calculate *RC* into two ways: (a) RC_{FWHM}: the product of ΔS_M^{pk} times the full temperature width at half maximum of the peak ($RC_{FWHM} = \Delta S_M^{pk} \cdot \Delta T_{FWHM}$) and (b) RC_{AREA}: the numerical integration of the area under the $\Delta S_M(T)$ curves, using the full temperature width at half maximum of the peak as the integration limits.

The temperature dependence of magnetic entropy change of the alloys under an applied magnetic field of 11 kOe is presented in Fig. 2, wherein the maximum values of $|\Delta S_M|$ for Gd1, Gd2, Gd3, Gd5, Gd8, Gd10, and Gd11 are 1.12, 0.91, 0.72, 0.75, 0.65, 0.52, and 0.37 J kg^{-1} K^{-1} respectively. At low applied magnetic fields, the Curie temperature can be identified as the temperature of the peak entropy change (T_{pk}) [34], the values of T_{pk} are presented in Fig. 3. It is observed that T_{pk} is displaced to higher temperatures with increasing Gd content. The evolution of Curie temperature in the binary $Gd_{100-x}Fe_x$ system follows a non-monotonic evolution, with a maximum for x = 70 at. % [35]. The increasing trend of Curie temperature with higher Gd content in FeGd alloys has been reported elsewhere [36,37]. In the alloy series studied in the present work, the presence of Cr and B in the alloy alters the position of the maximum, displacing it to lower Gd concentration.

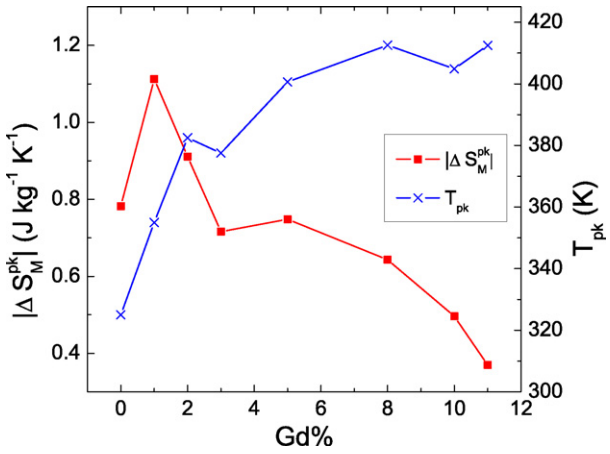

Fig. 3. Compositional dependence of $\left|\Delta S_M^{pk}\right|$ and T_{pk} of the as-spun ribbons.

The compositional dependence of $\left|\Delta S_M^{pk}\right|$ is shown in Fig. 3. The $\left|\Delta S_M^{pk}\right|$ initially increases with increasing Gd content up to 2 at.% Gd, following which it monotonically decreases. It has recently been shown that there is a correlation between the magnetic moment of the alloys and the magnetic entropy change values [38–40]. The magnetic moment of Fe was also reported to decrease with increasing Gd content in Fe–Gd alloys [36,37]. Hence there should be a decrease in ΔSM for higher Gd concentration.

To further study this relationship between $\left|\Delta S_M^{pk}\right|$ and the magnetic moment, the temperature dependence of magnetization was measured below the Curie temperature. For lower temperatures, magnetization was plotted as a function of $T^{3/2}$ to obtain low temperature spontaneous magnetization. As an example, the inset of Fig. 4 shows this procedure for Gd5. The values of $\left|\Delta S_M^{pk}\right|$ for the various alloys as a function of the spontaneous magnetization were plotted in Fig. 4, showing good agreement between the predicted linear dependence of the magnetic entropy change and the magnetic moment of the alloys. This shows that decrease in $\left|\Delta S_M^{pk}\right|$ with increasing Gd content can be ascribed to the decrease in spontaneous magnetization previously observed in Fe–Gd binary alloys [36,37].

When comparing the characteristics of different MCM from the published literature, one of the problems encountered is the variation in the experimental facilities available in different laboratories. In particular, $\left|\Delta S_M^{pk}\right|$ experimental values are usually reported for the maximum available magnetic field (H_{max}). Hence, the ratio $\left|\Delta S_M^{pk}\right|/H_{max}$ is sometimes quoted for performance comparison of magnetic refrigerants [10]. However, this is only useful if the field dependence of $\left|\Delta S_M^{pk}\right|$ for the compared materials is similar. If the field dependence of the compared materials is different, this ratio will offer unreliable information on the selection of MCM for a particular field value. Therefore the study of field dependence of MCE is of increasing interest since it allows comparison of the results obtained with different values of the maximum applied field.

The field dependence of magnetic entropy can be expressed as a power law of the magnetic field [41]:

$$\left|\Delta S_M\right| \propto H^n, \tag{2}$$

where the exponent n depends on H and T. It can be locally calculated as follows:

$$n = \frac{d \ln \left|\Delta S_M\right|}{d \ln H}. \tag{3}$$

In the particular case of $T = T_C$ or at the temperature of the peak entropy change, the exponent n becomes field independent [34]. In this case,

$$n(T_C) = 1 + \left(\frac{\beta - 1}{\beta + \gamma}\right), \tag{4}$$

where β and γ are the critical exponents [41].

The scaling of refrigerant capacity with field also controlled by the critical exponents of the material [42]:

$$RC_{FWHM} \propto H^{1+\frac{1}{\delta}}, \tag{5}$$

where the value of δ can be obtained from the Widom scaling relation, i.e., $\delta = 1 + \gamma/\beta$ [43].

The field dependence of $\left|\Delta S_M^{pk}\right|$ and RC for the Gd5 alloy are presented in Fig. 5. The curves for the other compositions are similar. By fitting $\Delta S_M^{pk}(H)$ and $RC\,(H)$ data to power laws, the exponents controlling these two magnitudes can be calculated. The exponent obtained for $\Delta S_M^{pk}(H)$ by this method is ~0.75 for Gd5 alloy. Theory predicts [42] that both RC_{FWHM} and RC_{AREA} should scale with field with the same value of exponent $(1+(1/\delta))$, this is in agreement with the experimental results (Fig. 5), which yield an exponent value of $1+(1/\delta)$ equals to 1.16 for both RC_{FWHM} and RC_{AREA}. The peak magnetic entropy change ($\left|\Delta S_M^{pk}\right|$) and RC of the studied alloys are presented in Table 1. Extrapolations to higher fields are performed using power laws from Eqs. (2) and (5) to enable comparison of the present results with those of other literature publications. Other typical MCM (Gd and $Gd_5Si_2Ge_2$) and Gd-based or Fe-based amorphous systems are also listed with their

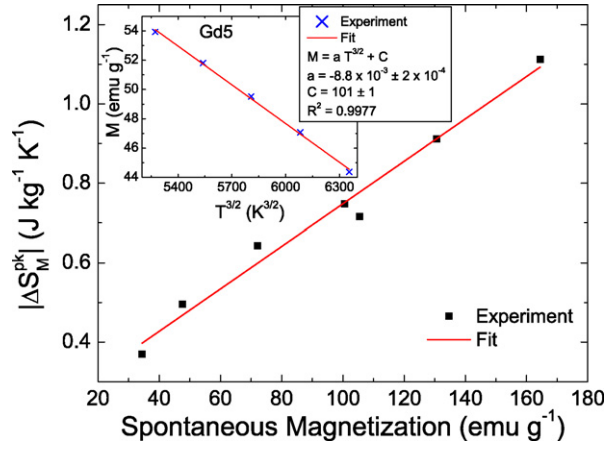

Fig. 4. Main panel: spontaneous magnetization dependence of $\left|\Delta S_M^{pk}\right|$. Inset: linear fit of M versus $T^{3/2}$ for Gd5 in the low temperature region.

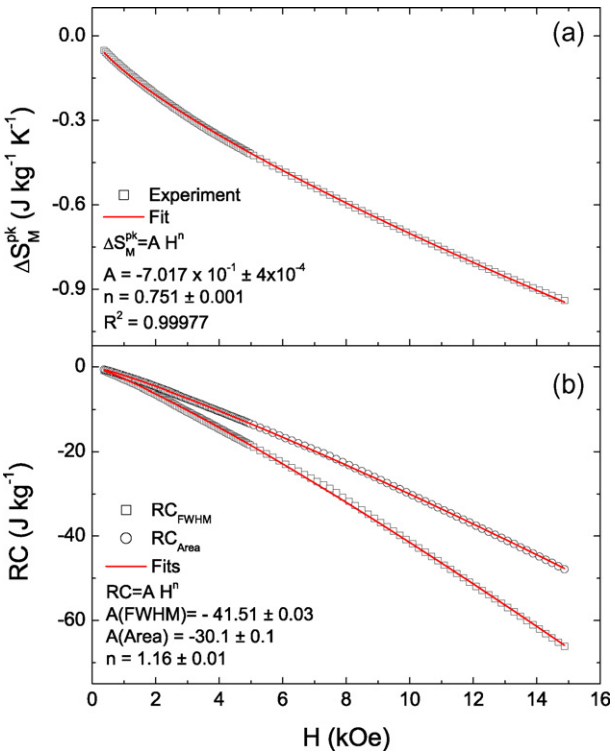

Fig. 5. Field dependence of (a) peak magnetic entropy and (b) refrigerant capacity for Gd5 alloy.

Table 1
Peak temperature and peak entropy change measured by VSM. Calculated refrigerant capacities, including extrapolations to fields of 1.5 and 5 T. For comparison, results for $Fe_{80}Cr_8B_{12}$ alloy of Ref. [21], $Fe_{88-2x}Co_xNi_xZr_7B_4Cu_1$ of Ref. [19], $(Fe_{100-x-y}Co_xCr_y)_{91}Zr_7B_2$-type alloy series of Ref. [18], Fe–Nb–B-type alloy series of Refs. [15,46], Gd of Ref. [47], $Gd_5Si_2Ge_2$ alloys of Ref. [13], $Gd_5Si_2Ge_{1.9}Fe_{0.1}$ of Ref. [14] and some Gd-based amorphous alloys of Refs. [22,24,27,48] are also presented.

Nominal composition	T_{pk} (K)	$\left\|\Delta S_M^{pk}\right\|$ ($J\,kg^{-1}\,K^{-1}$) VSM ($H = 1.1$ T)	$\left\|\Delta S_M^{pk}\right\|$ ($J\,kg^{-1}\,K^{-1}$) ($H = 1.5$ T)	$\left\|\Delta S_M^{pk}\right\|$ ($J\,kg^{-1}\,K^{-1}$) ($H = 5.0$ T)	RC_{FWHM} ($J\,kg^{-1}$) ($H = 1.1$ T)	RC_{FWHM} ($J\,kg^{-1}$) ($H = 1.5$ T)	RC_{FWHM} ($J\,kg^{-1}$) ($H = 5.0$ T)	RC_{AREA} ($J\,kg^{-1}$) ($H = 1.1$ T)	RC_{AREA} ($J\,kg^{-1}$) ($H = 1.5$ T)	RC_{AREA} ($J\,kg^{-1}$) ($H = 5.0$ T)	Ref.
$Fe_{79}Gd_1Cr_8B_{12}$	355	1.12	1.42	3.59	107	153	627	78	112	459	This work
$Fe_{78}Gd_2Cr_8B_{12}$	383	0.91	1.18	3.02	68	95	357	52	74	277	This work
$Fe_{77}Gd_3Cr_8B_{12}$	378	0.72	0.92	2.31	54	79	338	39	57	246	This work
$Fe_{75}Gd_5Cr_8B_{12}$	400	0.75	0.95	2.34	51	73	294	34	48	195	This work
$Fe_{72}Gd_8Cr_8B_{12}$	412	0.65	0.80	1.97	32	45	171	24	33	126	This work
$Fe_{70}Gd_{10}Cr_8B_{12}$	405	0.52	0.66	1.66	22	32	126	17	24	94	This work
$Fe_{69}Gd_{11}Cr_8B_{12}$	413	0.37	0.48	1.25	14	20	77	11	15	57	This work
$Fe_{80}Cr_8B_{12}$	328		1.07								[21]
$Fe_{83}Zr_6B_{10}Cu_1$	398		1.4						104		[20]
$Fe_{88}Zr_7B_4Cu_1$	295		1.32			166			121		[19]
$Fe_{82.5}Co_{2.75}Ni_{2.75}Zr_7B_4Cu_1$	398		1.41			166			119		[19]
$(Fe_{85}Co_5Cr_{10})_{91}Zr_7B_2$	320			2.8			240				[18]
$Fe_{80.5}Nb_7B_{12.5}$	363	0.72 (0.7 T)									[15]
$Fe_{81}Nb_7B_{12}$	363	0.7 (0.7 T)									[46]
Gd	294			10							[47]
$Gd_5Si_2Ge_2$	275			20						305	[13]
$Gd_5Si_2Ge_{1.9}Fe_{0.1}$	305			7						355	[14]
$Gd_{55}Co_{20}Al_{25}$	103			8.8						541	[22]
$Gd_{55}Ni_{25}Al_{20}$	78			8						640	[22]
$Gd_{40}Dy_{16}Al_{24}Co_{20}$	78			15.78						426	[48]
$Gd_{34}Dy_{22}Al_{24}Co_{20}$	75			9.64						518	[48]
$Gd_{51}Al_{24}Co_{20}Nb_1Cr_4$	100			9.48						611	[27]
$Gd_{53}Al_{24}Co_{20}Zr_3$	93			9.4			780			590	[24]
$Gd_{33}Er_{22}Al_{24}Co_{20}Zr_3$	52			9.47			714			574	[24]

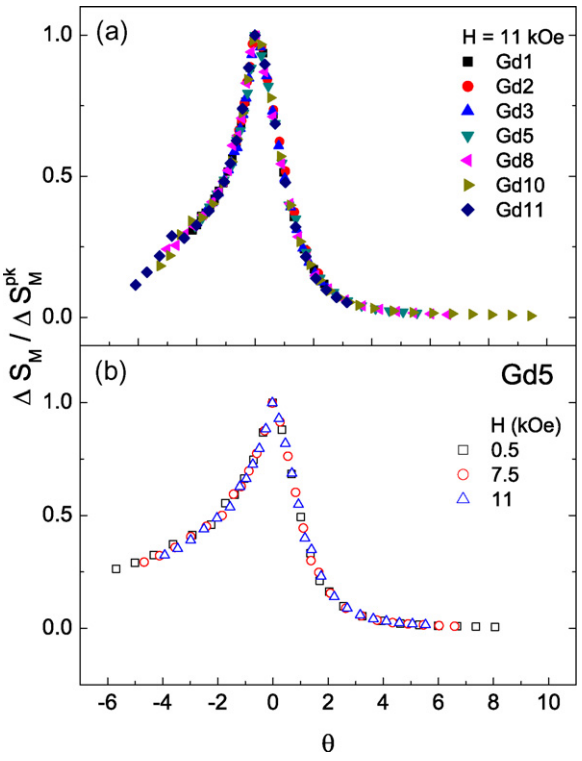

Fig. 6. Universal curves for (a) the studied alloys for $H = 11$ kOe and (b) Gd5 alloy for different maximum applied fields.

magnetocaloric properties in Table 1. When RC_{AREA} for the Gd1 alloy is extrapolated to an applied field of 5 T, it yields a value of 459 J kg^{-1}, which is a ~29% improvement over one of the best MCM, $Gd_5Si_2Ge_{1.9}Fe_{0.1}$ [14]. The T_{pk} values are higher for Fe–B–Cr–Gd alloys, although $\left|\Delta S_M^{pk}\right|$ and RC values are observed to be smaller than those of Gd-based amorphous alloys. Furthermore, Gd1 alloy increases $\left|\Delta S_M^{pk}\right|$ by ~33% with respect to $Fe_{80}B_{12}Cr_8$ amorphous alloy [21]. The RC_{FWHM} value for Gd1, which extrapolates to 153 J kg^{-1} for $H = 1.5$ T, is within 10% of $Fe_{82.5}Co_{2.75}Ni_{2.75}Zr_7B_4Cu_1$ (the best Fe-based MCM published so far with $RC_{FWHM} = 166$ J kg^{-1}), with a similar $\left|\Delta S_M^{pk}\right|$ value [19].

A phenomenological universal curve for ΔS_M has been proposed [41] to extrapolate magnetocaloric properties to magnetic fields and/or temperatures which are unavailable in various laboratories, enabling comparison of the performance of different MCM. Its construction is achieved by (a) the normalization of ΔS_M (T) curves with respect to their peak values (e.g., $\Delta S' = \Delta S_M(T)/\Delta S_M^{pk}$) and (b) rescaling the temperature axis as [44,45]:

$$\theta = \frac{T - T_C}{T_r - T_C}, \quad (6)$$

where T_r is the reference temperature selected in correspondence to $\Delta S(T_r) = 0.5\Delta S_M^{pk}$. The theoretical justification for this phenomenological construction of the universal curve has been previously reported [45]. The rescaled magnetic entropy change curves for different maximum applied magnetic fields of the as-spun Gd5 ribbon is shown in Fig. 6. It can be seen that the data for the series of alloys collapses onto the same universal curve.

4. Conclusions

The magnetocaloric response of $Fe_{80-x}B_{12}Cr_8Gd_x$ alloys was studied. Gd addition allows tuning the Curie temperature of the alloys and enhances the thermal stability of the amorphous phase against crystallization.

- Higher Gd content leads to a decrease in $\left|\Delta S_M^{pk}\right|$, the compositional dependence of $\left|\Delta S_M^{pk}\right|$ shows a linear dependence with magnetic moment of the alloys.
- The field dependence of $\left|\Delta S_M^{pk}\right|$ and RC is in good agreement with theoretical predictions of a power law dependence, the universal curve for the ΔS_M (T) is found to be applicable to this series of alloys.
- The RC observed in $Fe_{79}B_{12}Cr_8Gd_1$ amorphous alloys is ~29% larger than those of $Gd_5Si_2Ge_{1.9}Fe_{0.1}$ and within 10% of $Fe_{82.5}Co_{2.75}Ni_{2.75}Zr_7B_4Cu_1$.
- The tunable T_C around room temperature makes this alloy series potentially useful for the development of multimaterial layered magnetocaloric regenerators.

Acknowledgements

This work was supported by the US AOARD (AOARD-08-4018), program manager, Dr. R. Ponnappan, by the Spanish Ministry of Science and Innovation and EU FEDER (Projects MAT 2007-65227 and MAT 2010-20537), and the PAI of the Regional Government of Andalucia.

References

[1] A.M. Tishin, in: K.H.J. Bushow (Ed.), Handbook of Magnetic Materials, vol. 12, Elsevier, Amsterdam, 1999.
[2] K.A. Gschneidner Jr., V.K. Pecharsky, Annu. Rev. Mater. Sci. 30 (2000) 387.
[3] K.A. Gschneidner Jr., V.K. Pecharsky, A.O. Pecharsky, C.B. Zimm, Mater. Sci. Forum 315–317 (1999) 69.
[4] K.A. Gschneidner Jr., V.K. Pecharsky, Int. J. Refrig. 31 (2008) 945.
[5] C.E. Reid, J.A. Barclay, J.L. Hall, S. Sarangi, J. Alloys Compd. 207–208 (1994) 366.
[6] A.M. Tishin, Y.I. Spichkin, The Magnetocaloric Effect and its Applications, Institute of Physics Publishing, Bristol, 2003.
[7] E. Brück, J. Phys. D: Appl. Phys. 38 (2005) R381.
[8] V.K. Pecharsky, K.A. Gschneidner Jr., Int. J. Refrig. 29 (2006) 1239–1249.
[9] E. Brück, O. Tegus, D.T.C. Thanh, K.H.J. Buschow, J. Magn. Magn. Mater. 310 (2007) 2793–2799.
[10] A.M. Tishin, J. Magn. Magn. Mater. 316 (2007) 351–357.
[11] V.K. Pecharsky, K.A. Gschneidner Jr., in: H. Kronmüller, S. Parkin (Eds.), Magnetocaloric Materials, Novel Materials, Jonh Wiley & Sons Ltd., 2007.
[12] K.A. Gschneidner Jr., V.K. Pecharsky, A.O. Tsokol, Rep. Prog. Phys. 68 (2005) 1479.
[13] V.K. Pecharsky, K.A. Gschneidner Jr., Phys. Rev. Lett. 78 (1997) 4494.
[14] V. Provenzano, A.J. Shapiro, R.D. Shull, Nature 429 (2004) 853.
[15] I. Škorvánek, J. Kovác, Czech. J. Phys. 54 (Suppl. D) (2004) D189.
[16] V. Franco, J.S. Blázquez, M. Millan, J.M. Borrego, C.F. Conde, A. Conde, J. Appl. Phys. 101 (2007) 09C503.
[17] V. Franco, J.S. Blázquez, C.F. Conde, A. Conde, Appl. Phys. Lett. 88 (2006) 042505.
[18] F. Johnson, R.D. Shull, J. Appl. Phys. 99 (2006) 08K909.
[19] R. Caballero-Flores, V. Franco, A. Conde, K.E. Knipling, M.A. Willard, Appl. Phys. Lett. 96 (2010) 182506.
[20] V. Franco, J.S. Blázquez, A. Conde, J. Appl. Phys. 100 (2006) 064307.
[21] V. Franco, A. Conde, L.F. Kiss, J. Appl. Phys. 104 (2008) 033903.
[22] J. Du, Q. Zheng, Y.B. Li, Q. Zhang, D. Li, Z.D. Zhang, J. Appl. Phys. 103 (2008) 023918.
[23] Q.Y. Dong, B.G. Shen, J. Chen, J. Shen, F. Wang, H.W. Zhang, J.R. Sun, J. Appl. Phys. 105 (2009) 053908.
[24] Q. Luo, D.Q. Zhao, M.X. Pan, W.H. Wang, Appl. Phys. Lett. 89 (2006) 081914.
[25] H. Fu, M.S. Guo, H.J. Yu, X.T. Zu, J. Magn. Magn. Mater. 321 (2009) 3342.
[26] J. Chang, X. Hui, Z.Y. Zu, G.L. Chen, Intermetallics 18 (2010) 1132.
[27] Q. Luo, W.H. Wang, J. Alloys Compd. 495 (2010) 209.
[28] S. Tencé, E. Gaudin, B. Chevalier, Intermetallics 18 (2010) 1216.
[29] M.A. Richard, A.M. Rowe, R. Chahine, J. Appl. Phys. 95 (2004) 2146.
[30] J.A. Barclay, W.A. Steyert Jr., Active Magnetic Regenerator, US Patent No. 4,332,135 (1982).
[31] A. Rowe, A. Tura, Int. J. Refrig. 29 (2006) 1286.
[32] A. Lindsay Greer, Nature 366 (1993) 303.
[33] M.E. Wood, W.H. Potter, Cryogenics 25 (1985) 667.
[34] V. Franco, A. Conde, M.D. Kuz'min, J.M. Romero-Enrique, J. Appl. Phys. 105 (2009) 07A917.

[35] M. Sostarich, in: H.P.J. Wijn (Ed.), Liquid Quenched Alloys, Landolt-Börnstein Group III Condensed Matter: Numerical Data and Functional Relationships in Science and Technology, Springer-Verlag, Berlin, 1991, p. 247.
[36] K. Yano, E. Kita, K. Tokumitsu, H. Ino, A. Tasaki, J. Magn. Magn. Mater. 104–107 (1992) 131.
[37] K. Yano, Y. Akiyama, K. Tokumitsu, E. Kita, H. Ino, J. Magn. Magn. Mater. 214 (2000) 217.
[38] V. Franco, C.F. Conde, J.S. Blázquez, A. Conde, P. Svec, D. Janičkovič, L.F. Kiss, J. Appl. Phys. 101 (2007) 093903.
[39] Y. Wang, X. Bi, Appl. Phys. Lett. 95 (2009) 262501.
[40] R. Caballero-Flores, V. Franco, A. Conde, L.F. Kiss, to be published.
[41] V. Franco, J.S. Blázquez, A. Conde, Appl. Phys. Lett. 89 (2006) 222512.
[42] V. Franco, A. Conde, Int. J. Refrig 33 (2010) 465.
[43] B. Widom, J. Chem. Phys. 43 (1965) 3898.
[44] V. Franco, J.S. Blázquez, A. Conde, J. Appl. Phys. 103 (2008) 07B316.
[45] V. Franco, A. Conde, J.M. Romero-Enrique, J.S. Blázquez, J. Phys.: Condens. Matter 20 (2008) 285207.
[46] I. Škorvánek, J. Kovác, J. Marcin, P. Svec, D. Janičkovič, Mater. Sci. Eng. A 449–451 (2007) 460.
[47] S. Yu Dan'kov, A.M. Tishin, V.K. Pecharsky, K.A. Gschneidner Jr., Phys. Rev. B: Condens. Matter Mater. Phys. 57 (1998) 3478.
[48] L. Liang, X. Hui, G.L. Chen, Mater. Sci. Eng. B 147 (2008) 13.